NUMERICAL SIMULATION OF SUPERPLASTIC FORMING/DIFFUSION BONDING PROCESSES

O. Baldó, J. Díaz
Construcciones Aeronáuticas, S.A., Av. John Lennon s/n, 28906 Getafe, Spain

F. Martínez, F.J. Beltrán, A. Mateos, G.Rico
Principia, S.A., Velázquez 94, 28006 Madrid, Spain

Abstract

The paper reports on the results of four numerical simulations of superplastic forming processes carried out for Construcciones Aeronáuticas, S.A. (CASA) by Principia, S.A. in order to show the capabilities of general purpose finite element code ABAQUS/Standard in this field. Each problem corresponds to a real manufactured component for which experimental data are available.

The first simulation deals with the forming of two simple cylindrical Al-Li cups. Several axisymmetric computations were made with different assumptions for the friction between the metal sheet and the die. The second analysis corresponds to the fabrication of Ti-6Al-4V parts. The third problem is aimed at the simulation of the forming of an Al-Li component with general three dimensional geometry. Finally the last analysis shows the simulation of the forming of Ti-6Al-4V aircraft leading edge.

In all cases the main point of interest is the final geometry of the formed parts, mainly the distribution of thicknesses, that the program is able to predict.

Numerical results are compared with experimental measurements and, from the comparison, conclusions are extracted about modeling assumptions and the overall suitability of the program for this kind of applications.

1. Introduction

In order to increase the range of applicability of superplastic forming (SPF) within the aerospace industry, one of the main problems faced by engineers is the difficulty in predicting the thicknesses of the formed parts.

The process produces a very high level of strain in the material. Strains on the order of several hundred per cent are not uncommon. As a result, dramatic reductions of the original plate thicknesses usually take place. Except for very simple die geometries the distribution of thicknesses which results from a given process is difficult to predict using simplified procedures. This is specially true when due account is taken of the influence of certain factors, such as the friction between plate and die, which are not easy to control.

A common way to tackle this problem is to carry out an extensive experimental program. However, the high cost of physical testing and the number of tests required to determine the optimum pressure cycle and the resulting thickness distribution clearly justify the use of a numerical simulation tool. The role of numerical simulation is to reduce the time and costs needed to design a particular forming process. In this context, four problems were set up by CASA engineers in order to assess the capabilities of the general purpose finite element code ABAQUS/Standard (HKS, 1993); the numerical predictions were to be compared with results already obtained after considerable experimental work.

The rest of this paper is dedicated to the description of these four problems, the way in which they were modeled with ABAQUS/Standard and the comparison of analytical and experimental results. The experimental results were not communicated to the modellers prior to conducting the analyses; the calculations are therefore true predictions, as opposed to "postdictions".

2. Simulation I: Forming of two “top hat” Al-Li 8090

2.1 Description

The first case deals with the forming of two "top hat" Al-Li 8090 parts. Figure 1 shows the corresponding die geometry. The formed parts are basically two 370mm diameter circular cylinders with a rim, resembling "hats". They have a very simple geometry, with axial symmetry. The difference between them is the depth of the hat, which is 71mm in one case (50% top hat) and 114mm in the other (100% top hat).

The process starts from a 2.0mm plate which is clamped at a radius of 213mm with respect to the axis of revolution of the die by means of a sealing lip.

The forming takes place at a constant temperature of 530°C. At this temperature the creep of the alloy has been experimentally determined to follow a potential law of the type:

$$\sigma = A\,\dot{\varepsilon}^{m} \qquad (1)$$

where: σ = effective stress
$\dot{\varepsilon}$ = effective strain rate
A, m = material constants

The optimum strain rate for the material at the temperature of the process is approximately $10^{-3}s^{-1}$. The actual pressure cycles used to form the components were not given as part of the data for the simulation. The determination of an optimum pressure cycle for each of the components was part of the problem posed to Principia.

2.2 Finite element modelling

Taking advantage of the axial symmetry of the problem, 2D finite element models were used to simulate the forming process.

The material behavior was represented using a creep law of the type:

$$\dot{\varepsilon} = A\,\sigma^{n} t^{m} \qquad (2)$$

with m=0 and A and n adjusted to the given data.

The two forming process were simulated using a range of different values for the friction coefficient between the superplastic alloy and the die.

The plate was assumed to be fully restrained at the position of the sealing lips. This boundary condition was considered adequate since the study of local effects near the sealing lips was outside the scope of the benchmark.

As an average, the resulting models had about 900 degrees of freedom.

The ABAQUS capabilities for automatic amplitude control were used in order to obtain a pressure cycle compatible with the optimum strain rate given for the material.

Each computer run took a few hours of CPU time in an Silicon Graphics Indigo MIPS 3000 workstation.

2.3 Results

Figure 2 shows the evolution of the deformed shape during the simulation of the forming of the 100% top hat.

Figure 3 compares the analytical and experimental thickness profiles along sections of both components. The solid lines correspond to the experimental profiles and the shaded areas represent ABAQUS predictions for a particular value of the friction coefficient taking into account the initial tolerance for plate thickness (±0.1mm). It can be seen that a fairly good correspondence exists between analysis and experiment except for the area near the boundaries of the finite element model, where the discretization cannot represent local effects accurately.

As could be expected, the agreement between experiments and computations is better for the 50% top hat, in which deformation levels are smaller.

In figure 4 the optimum pressure cycle computed by ABAQUS is compared with the pressure cycles used in the experiment. Significant differences are apparent both in respect of the total time and the maximum pressure. The optimization algorithm used by ABAQUS produced shorter cycles with higher maximum pressures. Nevertheless, it is well known that the influence of the pressure cycle on the final predictions for thickness distribution is small; this was verified in all cases.

3. Simulation II: Forming of a Ti-6Al-4V aircraft component

3.1 Description

The second numerical simulation has a more of qualitative nature. The goal in this case was to test whether the program was able to predict the occurrance of a specific geometrical effect during the manufacturing process of a certain Ti-6Al-4V alloy component. This effect was unforeseen at the time of designing the process but was observed during prototype testing. Its nature will be discussed in the section on results.

The superplastic forming of this component is preceded by the diffusion bonding (DB) of a package of four 0.8mm plates. A picture of the actual part can be seen in figure 5. Figure 6 presents a schematic view of the idealized two dimensional process which was the object of the numerical simulation.

The process has two main stages. The first one is the diffusion bonding of the plate package. During this phase the plates are heated up to 925°C and subjected to a very high pressure, typically 2MPa, for a long period of time, around 2 hours. The plates become perfectly bonded everywhere except in the areas previously impregnated with an inhibiting chemical ("stop-off" chemical).

The simulation of this phase is of some interest because it helps in predicting potential defects (pores) in the bonded package.

After the first stage of diffusion bonding of the plates, the superplastic forming takes place. This is accomplished by injecting gas between the plates in the region which remained unbonded due to the presence of the stop-off material.

At the process temperature the behavior of the alloy can be represented by a law similar to (1). As in the previous problem, the pressure cycle for the second phase of the process was not supplied as part of the data. The pressure cycle for the superplastic forming had to be determined with the knowledge that the optimum strain rate for the alloy at the temperature of the process was $2x10^{-4}s^{-1}$.

3.2 Finite element modelling

The assumption of plane-strain conditions was considered acceptable. Friction was taken into account at all contacts. The bond in the areas where the stop-off material was not present was modelled. The edges of the model were considered clamped, without attempting to capture local effects in these areas. Once again, the automatic pressure control capability within ABAQUS was used in order to determine the optimum pressure cycle.

Figure 7 shows a view of the finite element model, which has over 4500 degrees of freedom. The computer run took approximately two days of CPU time using the same workstation as in the first benchmark.

5.3 Results

Figures 8 to 10 summarize the results of the simulation. Figure 8 shows the configuration of the plates at various stages during the diffusion bonding phase and figure 9 gives a sequence of deformed shapes in the superplastic forming of the product. The simulation was interrupted when a buckling instability appeared in the straight portion of the component. At this moment the computed geometry of the corrugated area was that shown in figure 10 together with the experimentally observed geometry.

As can be seen in figure 8, a small pore is left after bonding of the outer plates. For a more rigorous analysis, the mesh should probably be refined in the area.

It was mentioned earlier that the ability to predict a specific effect provided the motivation for conducting this analysis. The observation was that, from the beginning of the superplastic forming phase, the edge of the bonded region penetrates into the cavity of the dies (figure 9). The amount of penetration increases until the plates establish contact with the dies. From this moment onwards the penetration reduces but cannot be totally eliminated; consequently, the component is not formed properly.

The comparison with experimentally obtained shapes (figure 10) demonstrates that the simulation is able to capture well the actual phenomenon.

4. Simulation III. Forming of an Al-Li 8090 product

4.1 Description

The third problem proposed was of a three dimensional nature. The goal was to simulate the superplastic forming of an Al-Li 8090 product and to obtain a map of the resulting thicknesses.

Figure 11 shows the geometry of the die. It covers an area of 932x622mm^2 and its maximum depth is 60mm. The process starts from a 2.0mm plate and takes place at a temperature of 530°C. The material behavior is that already described in the first simulation.

As in previous cases, the questions posed included the determination of a pressure cycle compatible with the range of strain rates required for superplastic behavior.

4.2 Finite element modelling

Since the die has two planes of symmetry, only a quarter of the plate and die was included in the finite element model.

The contact with the die was simulated by means of rigid surface contact elements. The geometry of the die was represented using a Bezier surface defined by 3400 triangular patches. A friction coefficient was assigned to the contact.

The plate was clamped along the edges of the die and symmetry conditions were imposed at the other boundaries of the plate.

The model geometry is shown in figure 12. The mesh had a total of 10500 degrees of freedom. It should be said that, when the problem was solved as described above, the computer time requirements were extremely high: several weeks of CPU time in the same workstation mentioned earlier. The reason for this inordinate time requirements was not clear. However, the analysts have the feeling that the contact logic with Bezier surfaces may strongly benefit from some optimization.

4.3 Results

The results of the simulation are summarized in figures 13 to 15. Figure 13 shows the final deformed shape. In figure 14 two experimentally obtained thickness profiles along orthogonal directions are compared with ABAQUS predictions. The solid lines correspond to experimental results and the shaded areas represent analytical predictions, taking into account the tolerance for initial plate thickness (±0.1mm). It can be seen that the predictions are quite good, always within the margins of tolerance.

Note that, in this three dimensional case, it is extremely difficult to make "manual" or even intuitive predictions on what will be the shape of the final thickness distribution because it is highly dependent on the sequence in which the different areas of the plate come into contact with the die.

Finally, figure 15 compares the pressure cycle computed by ABAQUS with the actual pressure cycle used to form the component. Both cycles have the same shape and approximately the same maximum pressure.

5. Simulation IV: Forming of a Ti-6Al-4V leading edge

5.1 Description

The fourth problem proposed was also three dimensional. The goal was to simulate the forming of a Ti-6Al-4V aircraft leading edge with the aim of comparing the final geometric configuration and the thickness distribution with the experimental results. The forming, as the second simulation explained previously, has two stages.

In the first stage two different plates are subjected to a diffusion bonding process. The upper plate is 0.8mm of thickness while the lower is 4.4 and 3.0mm of thickness as is depicted in figure 16. The plates are previously heated up to 925°C. The bonding is accomplished applying a pressure of 2.1MPa upwards during nearly three hours. In this case the bonding takes place at the same time the plates are formed against an upper die. At the end of this stage the two plates are perfectly bonded except in those areas previously impregnated with an inhibiting chemical ("stop-off" chemical). The aim of this previous forming is to accomplish a corrugated longeron within the leading edge.

The second stage is properly the superplastic forming process. This is achieved applying a gas pressure between the two plates in the area where remains unbonded as a result of the first phase. The pressure cycle is not know and is obtained as a consequence of the numerical simulation keeping the strain rate of the alloy within an optimum range of $2\ 10^{-4}\ s^{-1}$.

5.2 Finite element modelling

Only a section between two parallel planes was included due to the symmetry of model. The contact with the two dies was modelled by means of rigid surface contact elements . The plate was clamped along the edges of the dies and symmetry conditions were imposed at two parallel planes.

The mesh has a total of 17000 degrees of freedom. The actual process took around three hours, while the simulation required four days of CPU time in the same workstation mentioned in previous sections.

5.3 Results

The results of the simulation are summarized in figure 17. This figure depicts the final deformed shape at the end of each stage. In the same figure it is represented the comparison between the experimentally obtained thickness profiles along the nose and the longeron and the numerical predictions. In this case the initial plate thickness tolerance is ±0.2mm. It can be seen that the predictions are again quite good.

6. Conclusions

The results of the four simulation problems presented here are very satisfactory and indicate that ABAQUS can be a very useful tool in the first stages of the design of a forming process. Such a tool allows making accurate predictions of the thickness reductions, timely detecting unforeseen phenomena and, generally, better understanding the mechanisms of a prototype process.

As in other fields, numerical simulation here can lead to substantial savings in the time needed to develop a particular fabrication sequence, reducing to a minimum the number of physical tests. The latter is specially true in the case of DB/SPF combined processes, where a large number of attempts may be necessary to define an appropriate package of plates with proper distribution of stop-off material.

On the other hand, it should be noted that the computer times involved, specially in three dimensional cases, may be significant. The finite element models used in the some of the simulations were not optimized in this sense and some reductions on the required CPU time could have been achieved with additional work. In any case, computer resources is a factor to bear in mind when dealing with this kind of simulations.

7. References

Hibbitt, Karlsson & Sorensen, Inc. (1993). "ABAQUS User's Manual". Version 5.3.

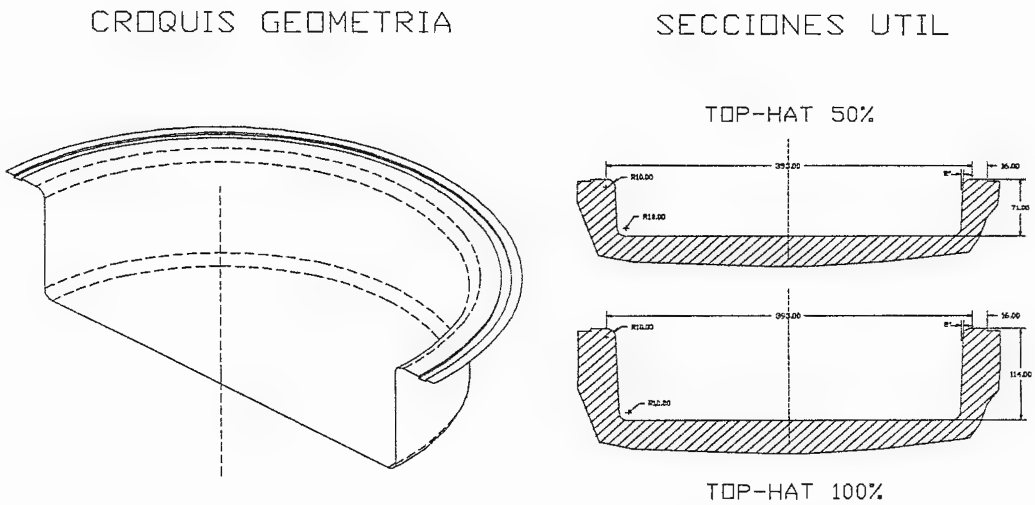

Figure 1. Simulation I. Geometry of "top hat" parts

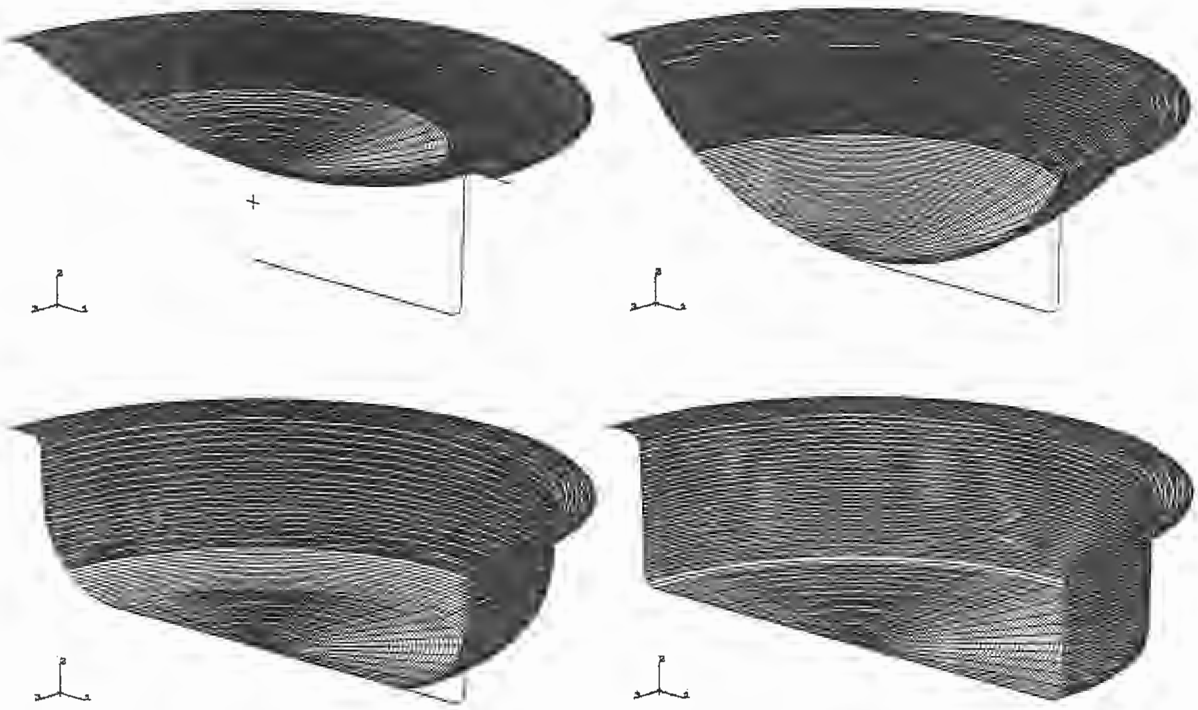

Figure 2. Simulation I. Sequence of deformed shapes in 100% top hat simulation

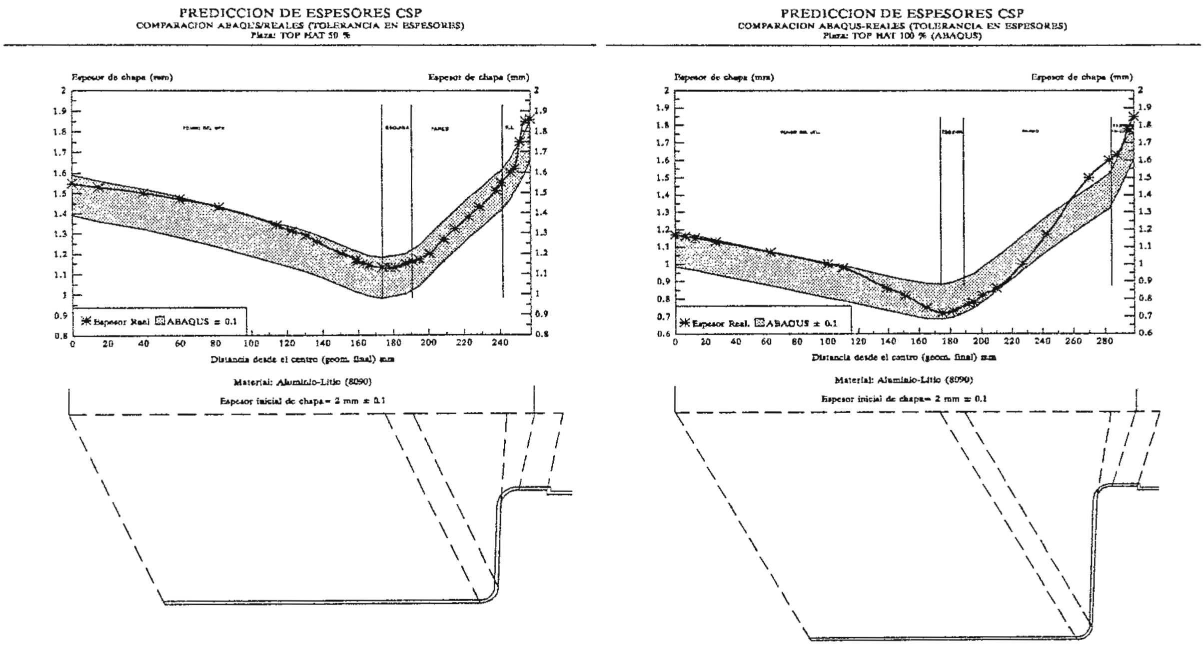

Figure 3. Simulation I. Comparison between analytical & experimental thicknesses

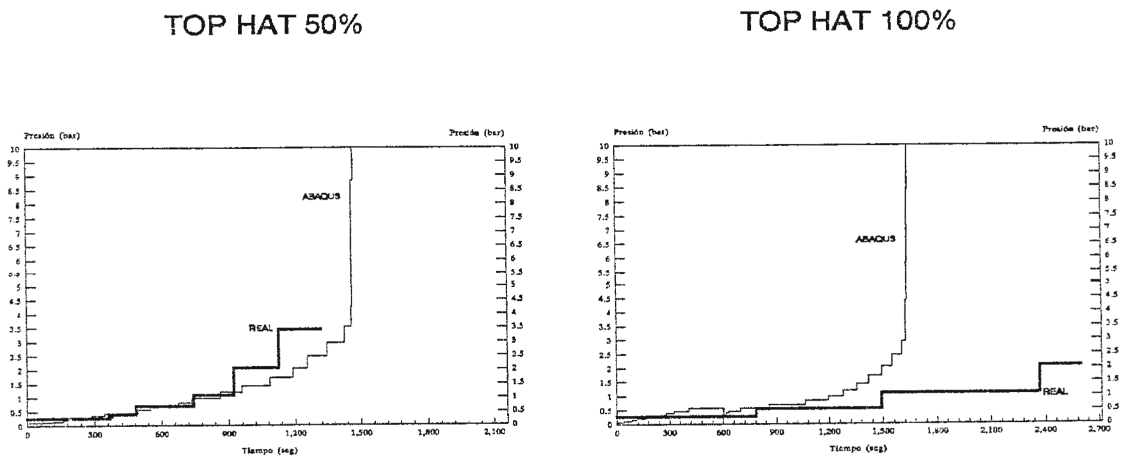

Figure 4. Simulation I. Comparison between analytical & experimental pressure cycles

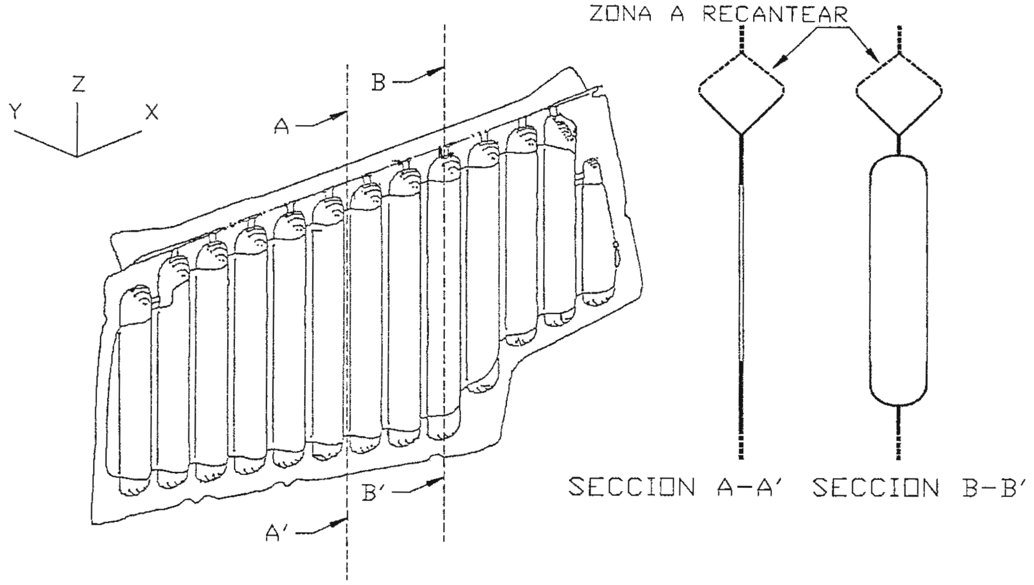

Figure 5. Simulation II. Geometry of real component

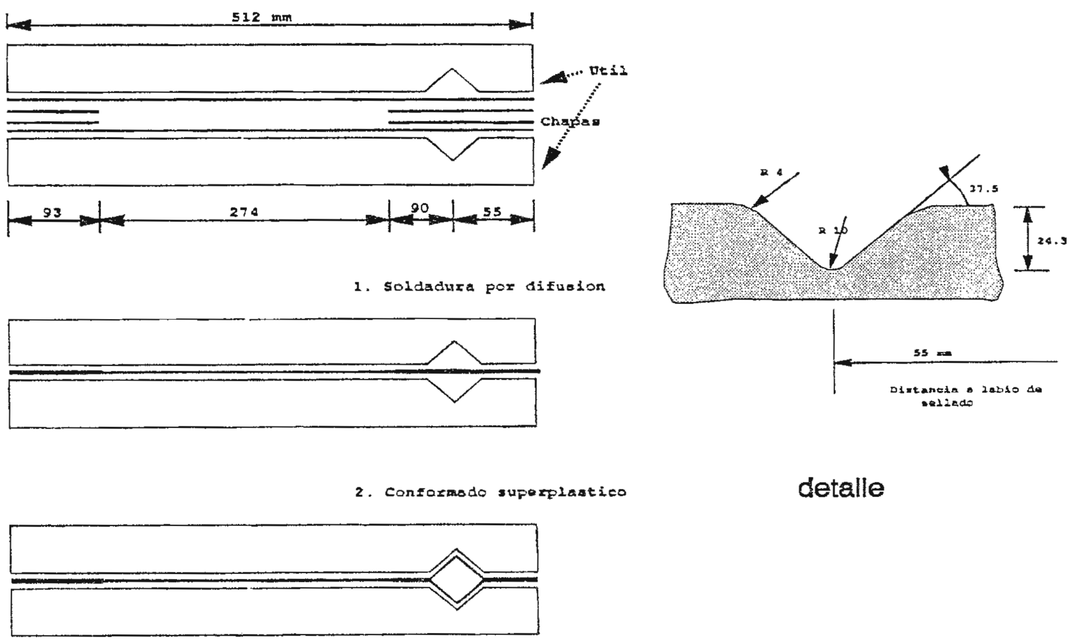

Figure 6. Simulation II. Idealized process

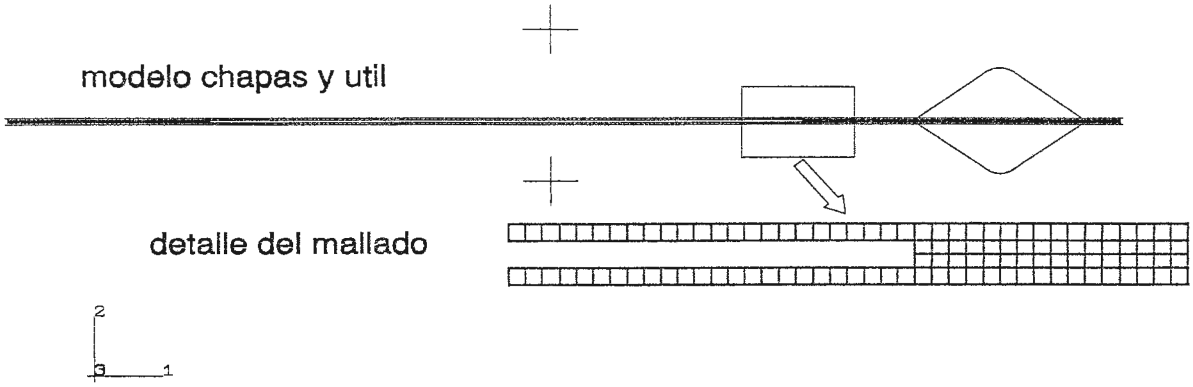

Figure 7. Simulation II. Finite element model

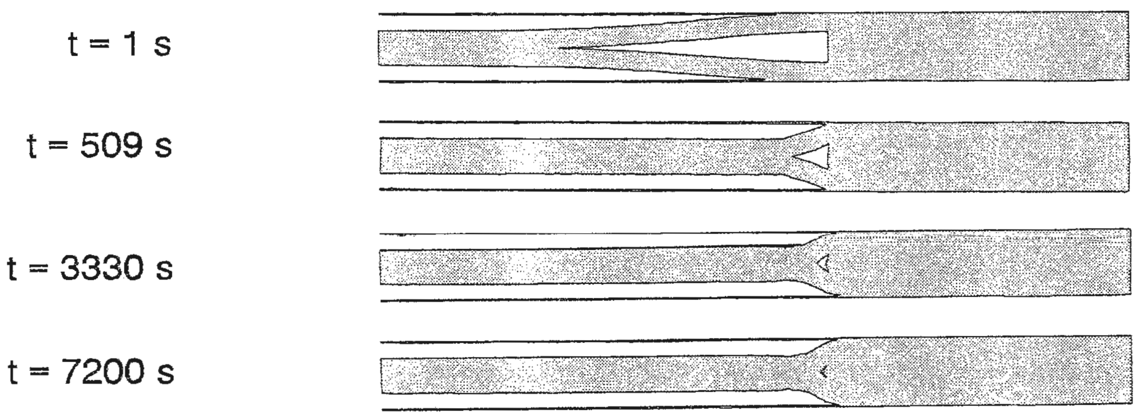

Figure 8. Simulation II. Deformed shapes in DB simulation

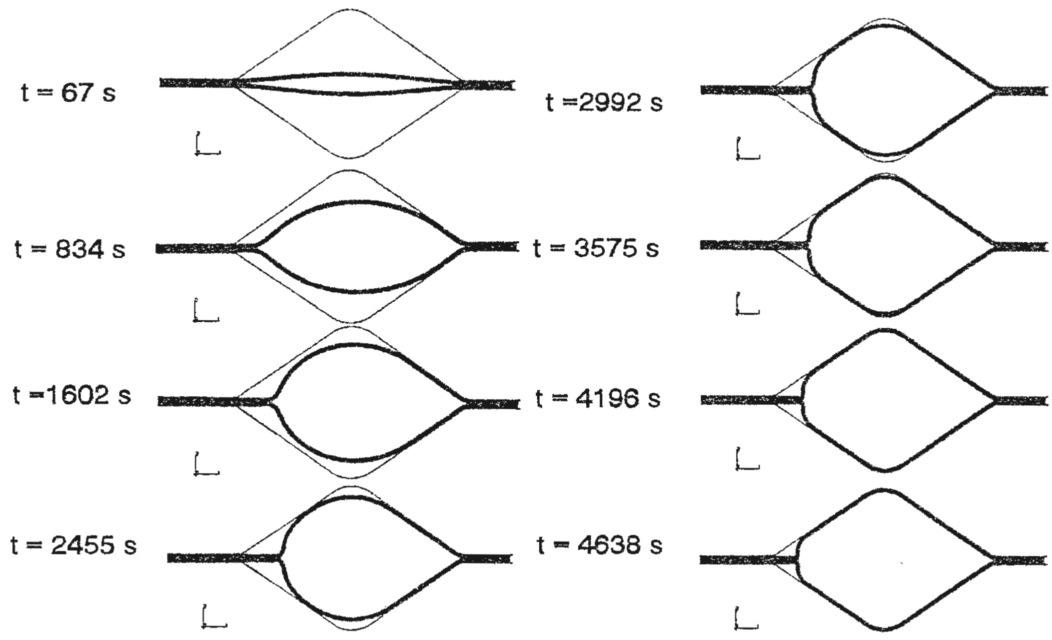

Figure 9. Simulation II. Deformed shapes in SPF simulation

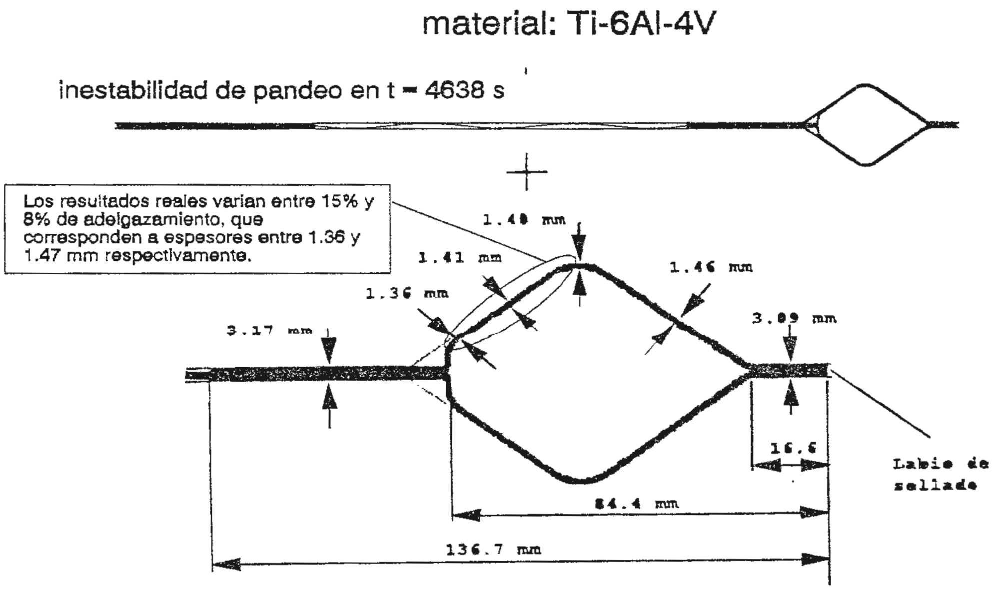

Figure 10. Simulation II. Comparison with experimental deformed shapes

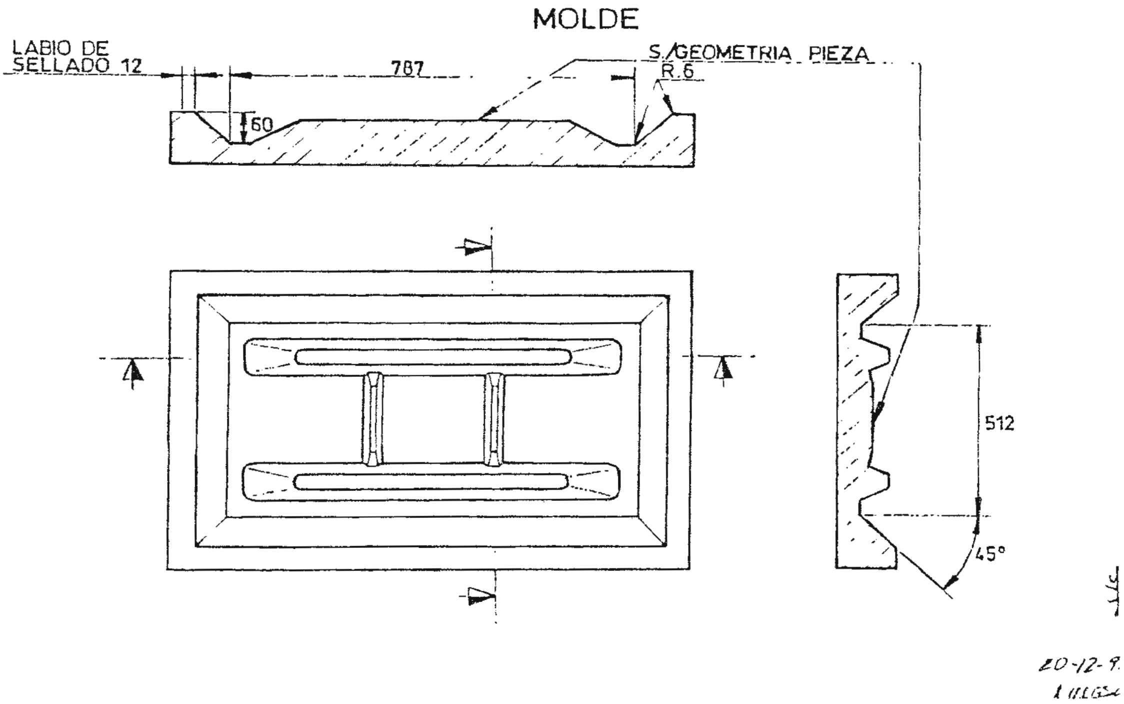

Figure 11. Simulation III. Geometry of die

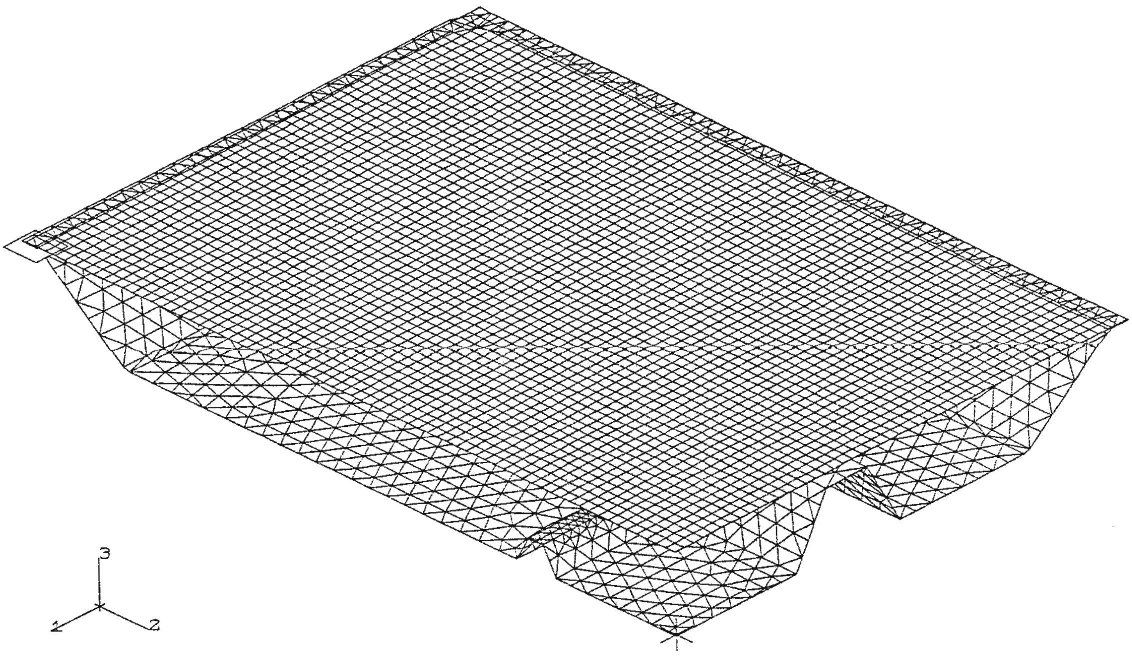

Figure 12. Simulation III. Finite element model

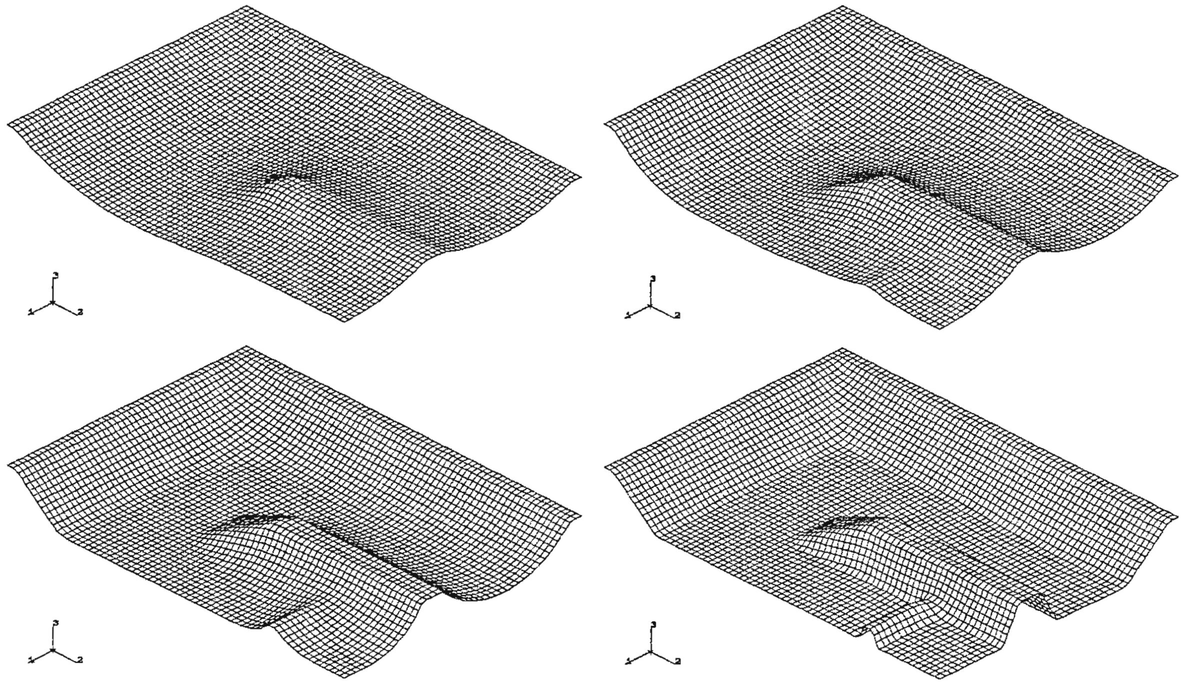

Figure 13. Simulation III. Deformed shapes

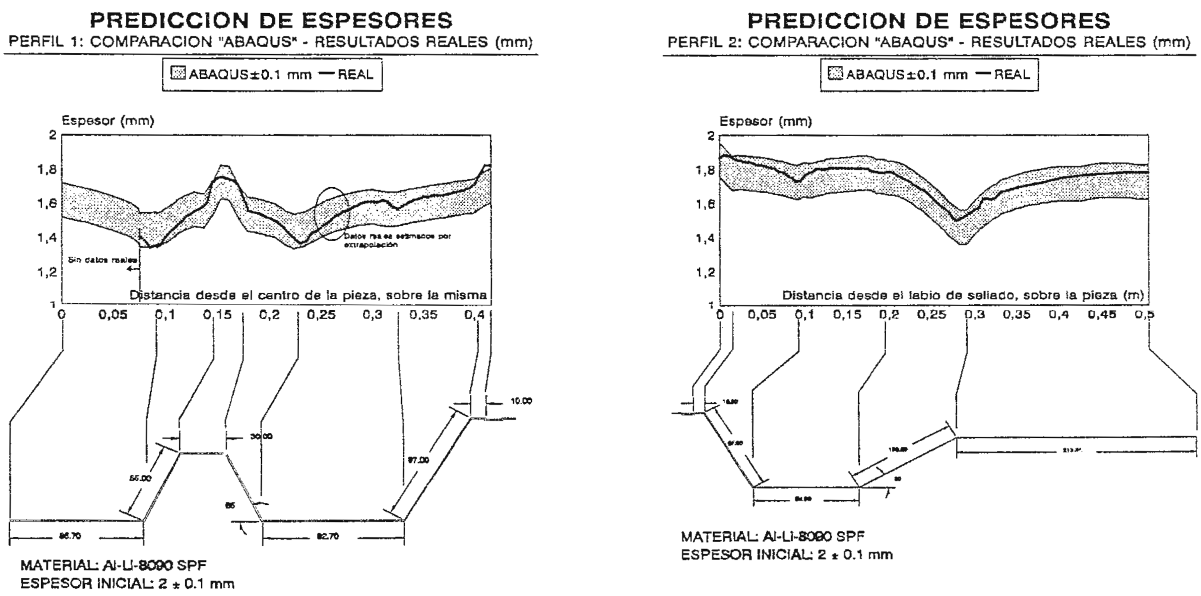

Figure 14. Simulation III. Profiles of thickness

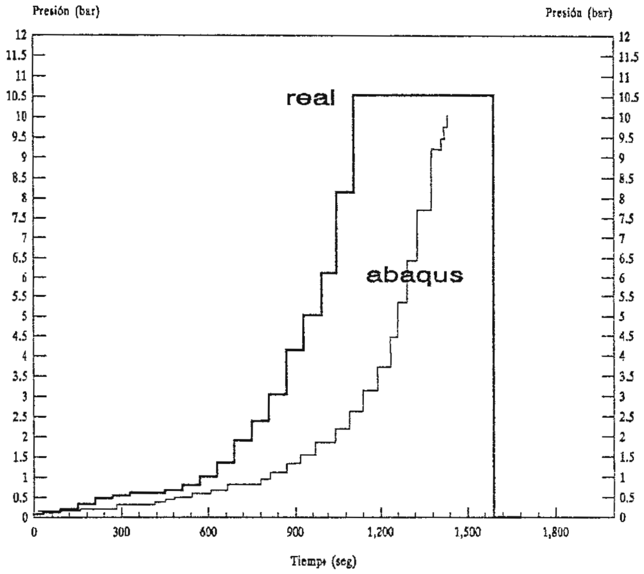

Figure 15. Simulation III. Pressure cycles

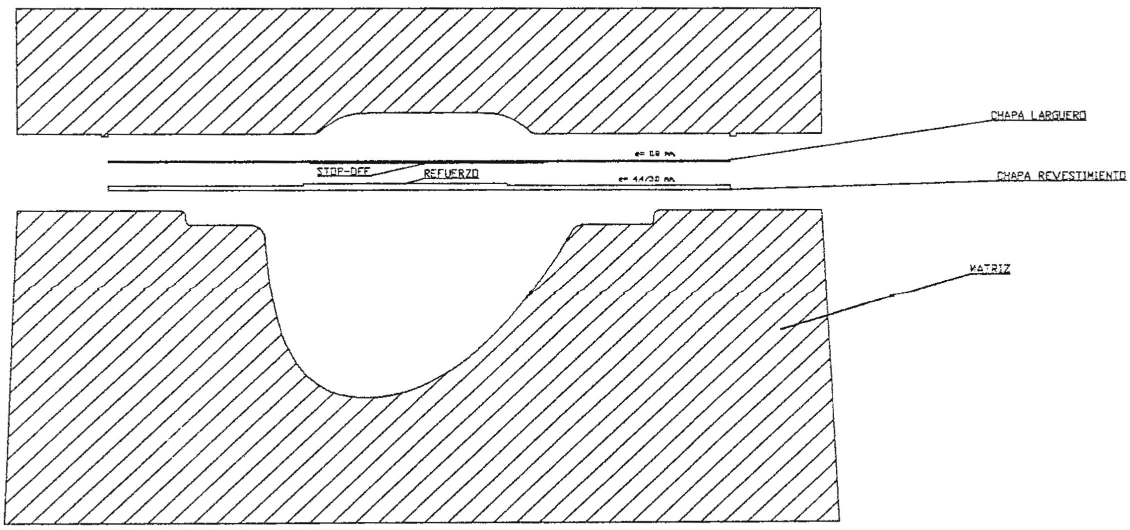

Figure 16. Simulation IV. Geometry of dies

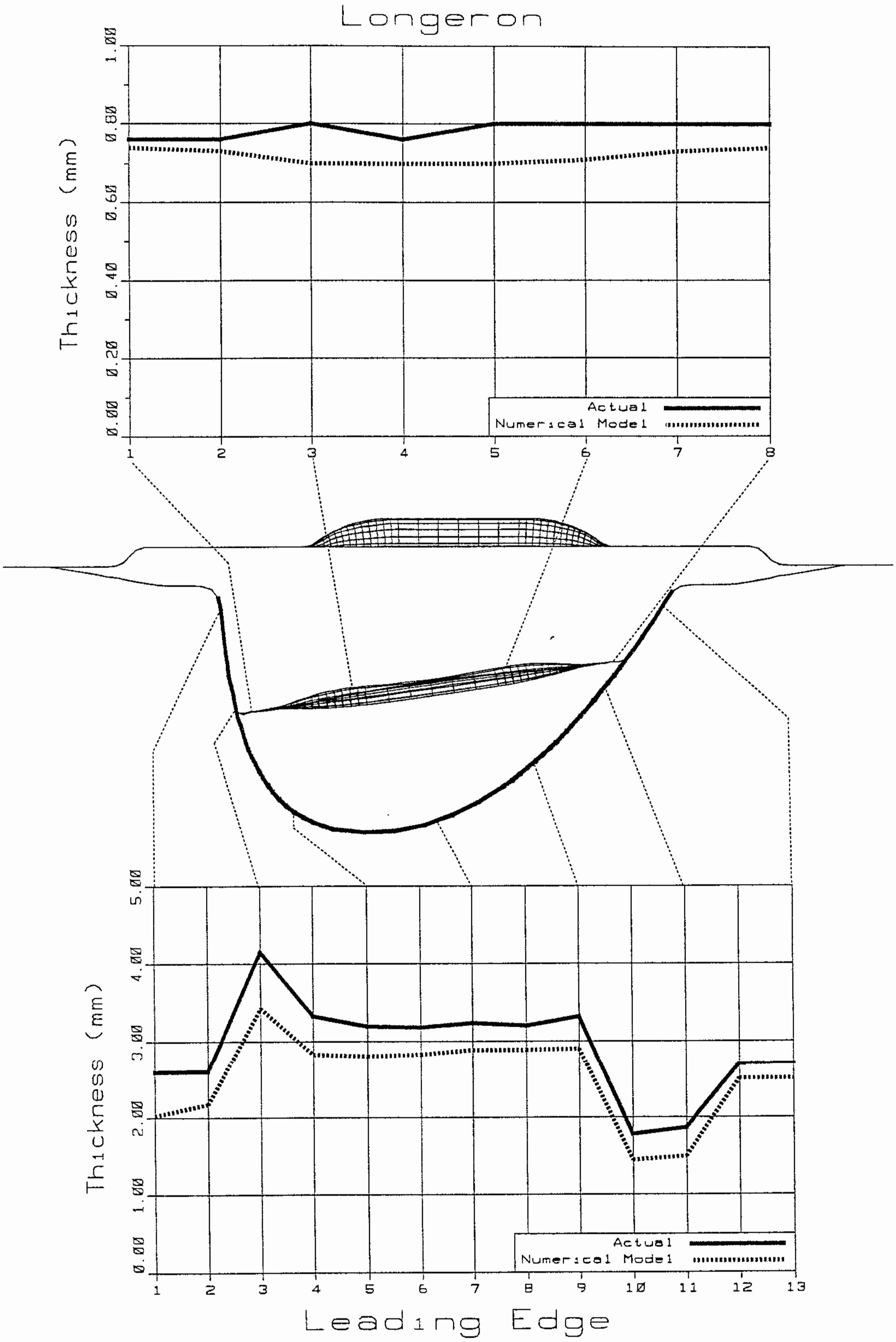

Figure 17. Simulation IV. Comparison Between analytical & experimental thicknesses